

Determining mRNA Capping with HILIC-MS on a Low-Adsorption Flow Path

Suitable for Agilent
1290 Infinity III LC

Limiting interfering interactions with iron surfaces using the Agilent 1290 Infinity II Bio LC System

Authors

Gerd Vanhoenacker,
Kris Morreel,
Stefanie Jonckheere,
Pat Sandra, and Koen Sandra
RIC group
President Kennedypark 6,
8500 Kortrijk, Belgium

Sonja Schneider and
Udo Huber
Agilent Technologies, Inc.

Abstract

The scientific leap taken in the development of therapeutic and prophylactic messenger ribonucleic acids (mRNA), and the increased public acceptance of the more recently available mRNA-related biopharmaceuticals, have propelled the search for new analytical methodologies for their characterization. Among these techniques are the determination of the incorporation efficiency of the cap structure onto the 5'-terminus of the mRNA. The measurement of this critical quality attribute (CQA) involves liquid chromatography/mass spectrometry (LC/MS) yet is hampered by the tendency of nucleic acids to adsorb to the iron surfaces of columns and instruments, especially when using hydrophilic interaction chromatography (HILIC) instead of ion pair reversed-phase (IP-RP) LC. As demonstrated in this application note, this phenomenon can be counteracted by opting for low-adsorption LC flow paths using a polyether ether ketone (PEEK)-lined HILIC column and an Agilent 1290 Infinity II Bio LC System.

Introduction

Worldwide successes in confining the COVID pandemic can largely be ascribed to the development of vaccines based on mRNA.¹ The approval of these landmark mRNA vaccines has paved the way for the full exploration of this technology both for prophylactic and therapeutic purposes. As a result, this evolution has urged the development of analytical methods to study various mRNA properties such as, among others, the 5'-cap structure and the proportion of capped mRNA.²⁻⁷

The mRNA cap is present at the 5'-end of the mRNA and consists of a 7N-methylguanosine that is 5'-5'-linked to the mRNA via a triphosphate ester (m7Gppp). However, small modifications might provide alternative cap structures, such as the Cap-1 structure resulting from an additional 2'-O-methylation of the first mRNA nucleotide being an adenosine (m7GpppAm), as shown in Figure 1.⁸

By preventing degradation, aiding cellular trafficking, and promoting the translation initiation and efficiency in eukaryotes, the cap is essential in yielding functional mRNA and so is considered a CQA.^{9,10} Within the production process, capping occurs during in vitro transcription of the mRNA (cotranscriptional capping) or, less commonly, is performed post-transcriptionally using a combination of enzymatic reactions. Whatever method is used, a small fraction of the mRNA pool will remain uncapped, displaying a 5'-terminus comprising 0 to 3 ester-linked phosphate groups.

Given the massive size of mRNA, determining the capping efficiency is typically performed by digesting the mRNA with ribonuclease (RNase) prior to analyzing the 5'-terminal fragments (Figure 1). Digestion might occur either on the single-stranded mRNA using RNase A or T1, or on an mRNA/DNA hybrid using the double-strand specific RNase H.

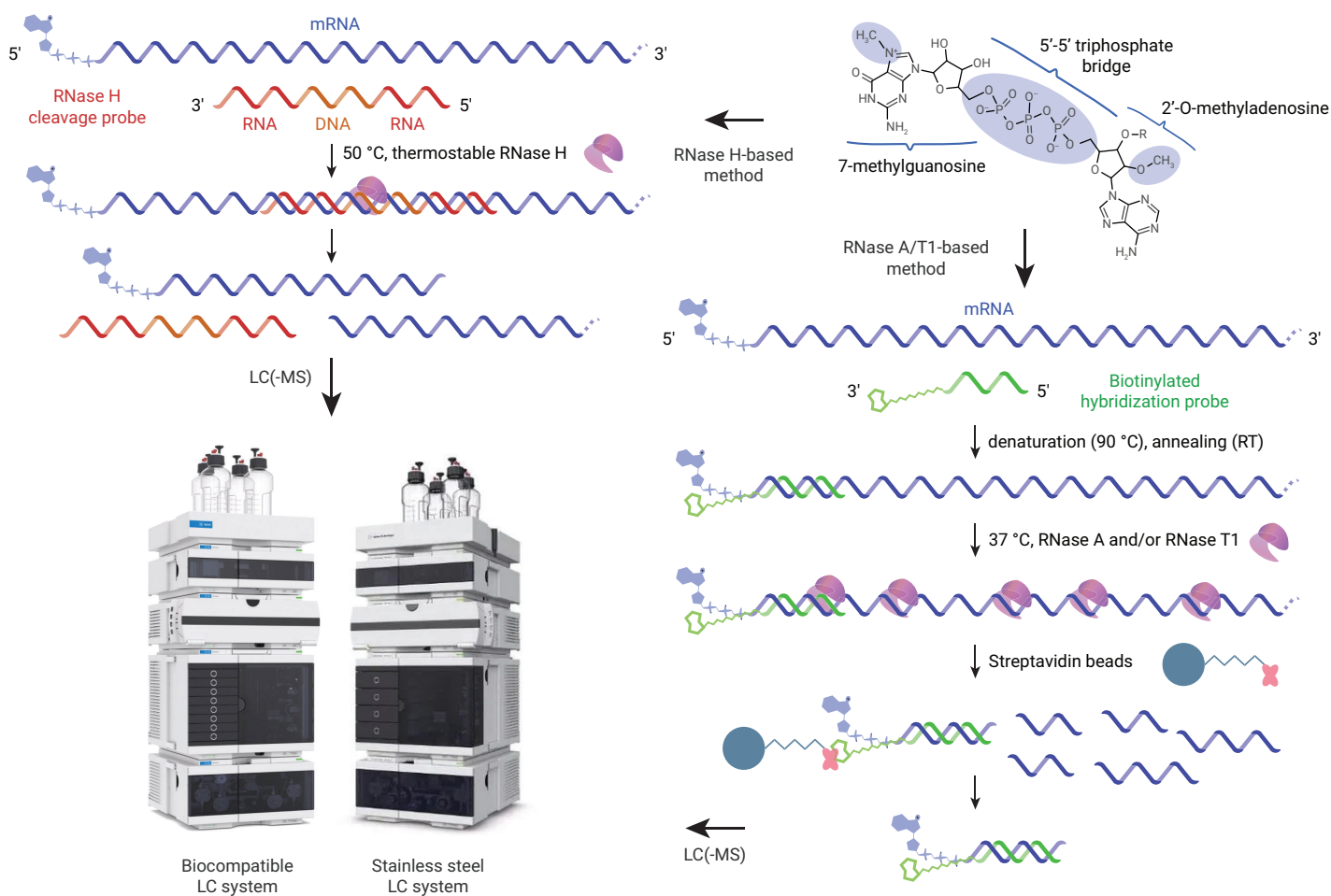


Figure 1. Capping efficiency analysis workflow. Most of the 5'-termini of eukaryotic mRNA bear a cap structure consisting of a 7-methylguanosine (m7G) that is 5'-5'-linked to a 2'-O-methyladenosine (Am) via a triphosphate ester (m7GpppAm, which can be abbreviated to Cap-1; upper right). Variations on this cap structure, especially with respect to the methylation sites, also occur. The mRNA cap can be isolated using either the DNA/RNA duplex-dependent RNase H (left) or via RNA single-strand dependent RNase A and/or T1 (right) prior to LC/MS analysis. RT: room temperature. See the Experimental section for further explanation.

While fragmentation of the phosphodiester bond by RNase A or T1 yields a 5'-terminal fragment retaining the phosphate group at its 3'-end, the latter position is not phosphorylated when RNase H is employed. Both strategies involve a hybridization probe. When using RNase A or T1, this probe protects the mRNA 5'-terminus against digestion.⁵ Alternatively, the probe directs RNase H cleavage towards its hybridization site near the 5'-terminus.^{2,3} Regardless of the method used, the resulting 5'-terminal mRNA fragments are analyzed via LC coupled to MS.

The many negatively charged phosphate moieties of nucleic acids offer at least two challenges when being analyzed via LC/MS: iron surface adsorption and iron complexation. Whereas the former problem (adsorption to the stainless-steel surfaces present in the LC flow path) will induce peak broadening and loss, the latter issue is especially detrimental to the detection sensitivity when using MS. Noticeably, as numerous metal ions, especially sodium and potassium ions, are electrostatically attracted by nucleic acids, the MS signal is distributed across many charge states and adducts.⁴ By thorough cleaning of the LC/MS flow path and avoiding glassware and glass surfaces during the analysis and handling of nucleic acids, the contribution of adducts to the MS signal can be partially circumvented. Furthermore, analyzing nucleic acids via IPRP-LC/MS affords less metal surface adsorption owing to the neutralization of the nucleic acids by the N-alkyl amine ion-pairing reagent (IPR). This ion-pairing effect drives the retention mechanism in IPRP as the IPR bears a hydrophobic moiety that will be retained by the apolar stationary phase.⁴ However, while metal adsorption is seemingly solved by IP-RP LC/MS, other hurdles come into play, such as the high concentrations of IPR and counterions that contaminate and affect the LC/MS instrument. As a cleaner and more sustainable alternative, HILIC is increasingly preferred for the LC/MS analysis of nucleic acids.^{11–13} As HILIC separation involves the partitioning of the "naked" nucleic acids between an apolar mobile phase and a water-layered polar stationary phase, stainless-steel flow paths will readily interfere with the separation. To deal with this metal surface adsorption, LC instruments and columns from which iron is eliminated, or metal surfaces deactivated or covered with, for example, PEEK, have been developed.

This application note describes the determination of mRNA capping following probe-guided RNase digestion and LC/MS analysis of the resulting 5'-containing mRNA oligonucleotides using a PEEK-lined diol HILIC column installed on a 1290 Infinity II Bio LC System and hyphenated with an Agilent 6545 LC/Q-TOF. The benefit of using low-adsorption flow paths is described and illustrated.

Experimental

Critical materials

Ammonium acetate (LC/MS grade) was acquired from Merck. Water (ULC/MS CC/SFC grade) and acetonitrile (HPLC-S grade) were supplied by Biosolve. Thermostable RNase H was purchased from New England Biolabs and RNase A from Thermo Fisher Scientific. Hybridization probes were ordered from Integrated DNA Technologies. Dynabeads MyOne Streptavidin C1 were purchased from Invitrogen. RNA Resolution Standard was received from Agilent Technologies and CleanCap Firefly Luciferase (Fluc) mRNA from TriLink BioTechnologies. The 1.2 kilobase (kb) mRNA was synthesized in-house by in vitro transcription from linearized plasmid DNA.

Sample preparation

The RNA resolution standard was dissolved in 1 mL of water/acetonitrile 50/50 (v/v). Further 10 and 50-fold dilutions were done in water/acetonitrile 50/50 (v/v).

Two procedures were employed for mRNA cap isolation (Figure 1). The first procedure was performed as described by Liao³ and starts with the hybridization of the probe to an mRNA region near the 5'-terminus followed by thermostable RNase H-targeted cleavage of the mRNA in this RNA/probe duplex region at 50 °C for 45 minutes. A second procedure was based on the methods described by Nwokeoji *et al.*⁵ and Wolf *et al.*⁶, in which hybridization of the probe protects the mRNA 5'-terminus from degradation by RNase A, which proceeded for 1 hour at 37 °C. Because the different mRNA fragments resulting from RNase A digestion (covering a mass range from monomers up to oligomers) would readily mask any eluting 5'-terminal mRNA fragment, a prior isolation of the latter fragments is necessary. For this purpose, the hybridization probe contained a biotin label that enabled purification of the probe/5'-terminus duplexes through the use of streptavidin-loaded magnetic beads according to the manufacturer's protocol.

Instrumentation and method

Two Agilent LC systems were used: the 1290 Infinity II LC (stainless steel - SST) and the 1290 Infinity II Bio LC (biocompatible - BIO). Details of both configurations can be found in Table 1 and method parameters are summarized in Table 2. Data were acquired and processed in Agilent OpenLab CDS version 2.6, Agilent MassHunter for Data Acquisition B 10.0, and Agilent MassHunter Qualitative Analysis B.07.00.

Table 1. Details of the LC and MS systems used.

	SST LC System	BIO LC System
Pump	Agilent 1290 Infinity II High-Speed Pump (G7120A)	Agilent 1290 Infinity II Bio High-Speed Pump (G7132A)
Autosampler	Agilent 1290 Infinity II Multisampler (G7167B) with integrated sample thermostat	Agilent 1290 Infinity II Bio Multisampler (G7137A) with integrated sample thermostat
Column Compartment	Agilent 1290 Infinity II Multicolumn Thermostat (G7116B) with Agilent InfinityLab Quick Connect heat exchanger, standard flow (G7116-60015)	Agilent 1290 Infinity II Multicolumn Thermostat (G7116B) with Agilent InfinityLab Quick Connect Bio heat exchanger, standard flow (G7116-60071)
Detector	Agilent 1290 Infinity II DAD (G7117B)	Agilent 1290 Infinity II DAD (G7117B)
Flow Cell	Agilent InfinityLab Max-Light Cartridge Cell, standard, 10 mm (G4212-60008)	Agilent InfinityLab Max-Light Cartridge Cell, LSS, 10 mm (G7117-60020)
Q-TOF MS	Agilent 6545 LC/Q-TOF (G6545A)	Agilent 6545 LC/Q-TOF (G6545A)

Table 2. LC method parameters.

Parameter	Value
Columns	Diol-HILIC column, 2.1 × 100 mm, 1.9 µm Stainless-steel version and PEEK-lined version
Flow Rate	0.35 mL/min
Mobile Phase	A) 20 mM ammonium acetate in water/acetonitrile 20/80 (v/v) B) 20 mM ammonium acetate in water/acetonitrile 80/20 (v/v)
Gradient 1	Time (min) %B 0 10 17 55
Gradient 2	Time (min) %B 0 0 21 55
Injection	2 µL
Needle Wash	Flush port, 3 s, water/acetonitrile 75/25 (v/v)
Autosampler Temperature	8 °C
Column Temperature	40 °C
Detection DAD	260/4 nm, reference 360/40 nm, peak width > 0.013 min (20 Hz), collect all spectra

Table 3. LC method parameters, for detection MS.

Parameter	Value
Detection MS	ESI, negative ionization, diverter valve bypassed*
Source	
Drying Gas Temperature	300 °C
Drying Gas Flow	8 L/min
Sheath Gas Temperature	350 °C
Sheath Gas Flow	10 L/min
Nebulizer Pressure	35 psi
Capillary Voltage	4,500 V
Nozzle Voltage	1,800 V
Fragmentor	200 V
Skimmer	65 V
Acquisition	
Acquisition Mode	Extended dynamic range (2 GHz)
Mass Range	m/z 400 to 3,200
Scan Rate	3 Spectra/s
Reference Mass	Disabled

*Diverter valve was bypassed to prevent potential non-specific interactions with stainless-steel components of the valve hardware.

Results and discussion

Prior to mRNA capping analysis, an RNA resolution standard composed of a 14, 17, 20, and 21-mer was subjected to the diol HILIC phase present in a stainless-steel or PEEK-lined housing installed on a 1290 Infinity II Bio LC system (Figure 2). On the stainless-steel column, the initial response for the oligonucleotides is disappointingly low, and increases gradually with subsequent injections to reach a steady state after five injections. However, even after conditioning, the peak height and area are much lower compared to that obtained on a PEEK-lined column, where maximum peak intensity is obtained with the first injection. These observations are in line with the findings recently noted by Lardeux *et al.*¹⁴ Next to the optimal intensity, peak shape and resolution are also dramatically better on the PEEK-lined column. The recovery for diluted solutions is furthermore greatly enhanced using this column. As shown in Figure 2, upon 50-fold dilution, all oligonucleotides are clearly detected, with the excellent peak shape maintained. On the stainless-steel column, however, this level can no longer be detected. Even a 10-fold dilution of the RNA resolution standard is problematic with this hardware.

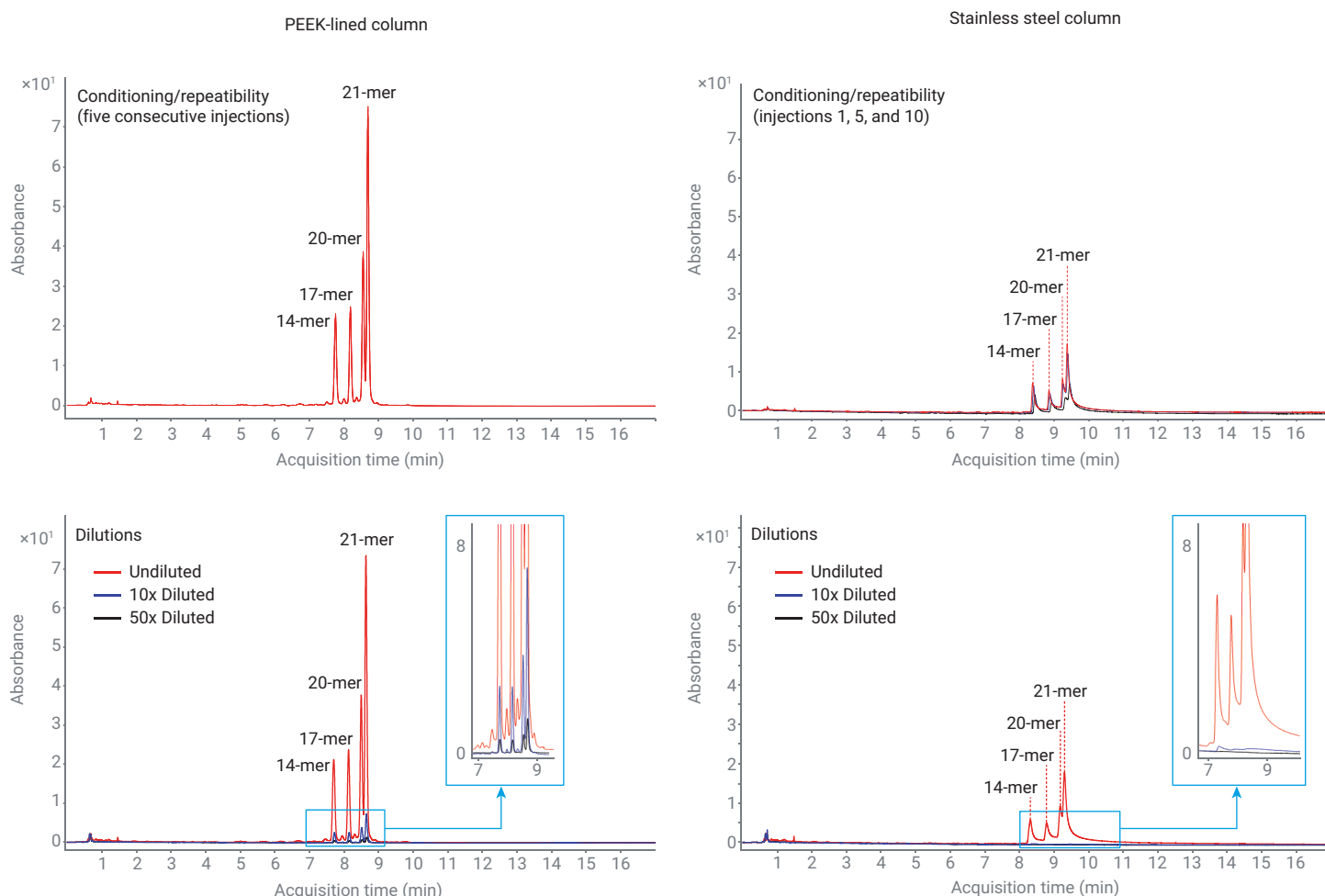


Figure 2. HILIC-DAD analysis (UV 260 nm) of the RNA resolution standard on a PEEK-lined column (left) and stainless-steel column (right) installed on an Agilent 1290 Infinity II Bio LC System. Gradient 1 (Table 2) was applied. Upper pane shows multiple injections of the same solution on brand new columns; lower pane shows the undiluted, 10, and 50-fold diluted RNA resolution standards.

Beyond column hardware, the impact of the LC instrument (stainless steel versus biocompatible) was evaluated using the RNA resolution standard. Figure 3 plots the peak area and tailing factor obtained for all instrument/column combinations and reveals that the effect of column hardware is greater than the system hardware. This is in accordance with earlier findings^{14–18} and can be explained by the fact that the column (tube and frits) represents 70% of the accessible

surface and that analyte residence time in the column largely exceeds the time in the LC instrument. Nevertheless, the impact of the system, although less obvious, cannot be neglected. To maximize chromatographic performance, it is therefore recommended to choose a configuration devoid of iron components in the sample flow path (i.e., a PEEK-lined column and a 1290 Infinity II Bio LC).

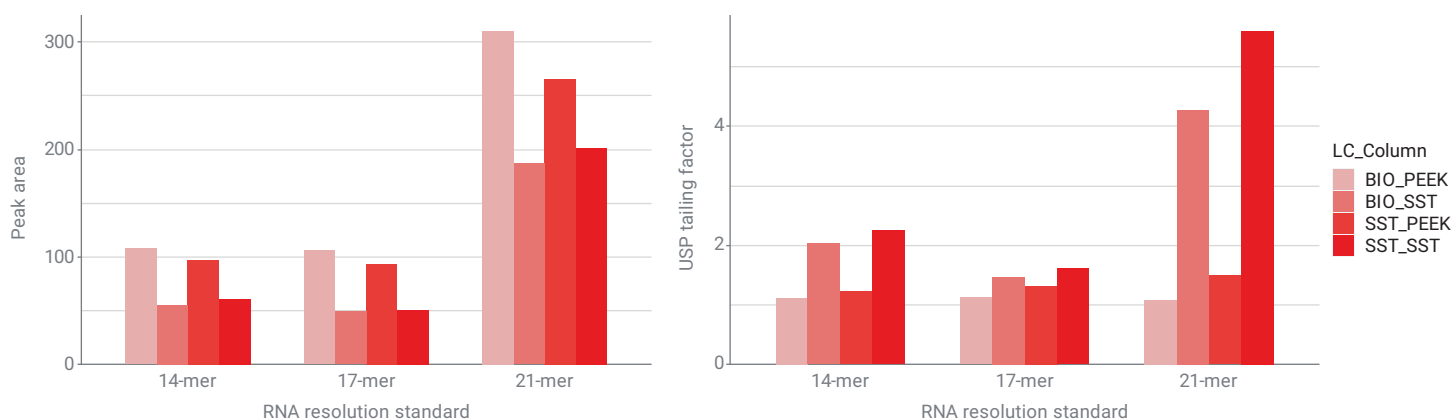


Figure 3. Peak area and USP tailing factor retrieved from the analysis of the RNA resolution standard on HILIC-DAD (UV 260 nm) using various instrument (BIO and SST) and column combinations (PEEK and SST). The 20-mer is excluded from the graphs as the marginal resolution (on SST configurations) disturbs the accurate calculation of peak area and tailing.

The disturbed peak shapes and intensities during HILIC analysis of nucleic acids in the presence of stainless-steel surfaces are due to the electrostatic interactions of the negatively charged phosphate ester moieties and the iron surfaces. Such interactions might especially affect the analysis of the 5'-termini of in vitro transcribed mRNA, where a high number and diverse set of phosphate moieties are encountered.

Procedures for the isolation of the mRNA 5'-termini are based on the use of hybridization probes, either to direct the cleavage to the mRNA site that is hybridized to the probe (e.g., by way of RNase H) or to protect the 5'-terminal regions from mRNA digestion by single-strand cutters such as RNase A or T1 (Figure 1). Whereas RNase H cleavage yields single-stranded 5'-terminal fragments with a non-phosphorylated 3'-end, RNase A and T1 provide fragments having either a 3'-phosphate ester or cyclic 2',3'-phosphodiester moiety. Furthermore, the RNase A/T1 procedure results in 5'-terminal fragments that are still annealed to the hybridization probe. The 5'-termini isolated via both approaches were subjected to HILIC-MS using either a stainless-steel or iron-free LC flow path (column and system). A 1.9-kb-long (Fluc mRNA) and a 1.2-kb-long mRNA were employed for the RNase H- and RNase A-dependent methods, respectively.

In the case of the RNase H-derived 5'-terminal mRNA fragments, the benefit of using an iron-free rather than a stainless-steel LC flow path is immediately clear when comparing the HILIC-MS base peak chromatograms (Figure 4). While readily measurable by way of the low-adsorption flow path, the capped 5'-terminus, referred to as m7GpppAm (N)_{25'}, is not observed using a stainless-steel configuration. As displayed in Figure 4, the full MS spectrum of this capped peak is rather complex, showing two skewed distributions of *m/z* peaks, each distribution representing a particular charge state (−5 and −6) and containing *m/z* peaks for various isotopes and adducts. This spreading of the detection signal across many *m/z* peaks turns MS into a precarious detection technique. A complex mass spectrum is also recorded for the hybridization probe which, being shorter and lacking 2'-hydroxy ribosyl moieties, elutes earlier than the capped fragment m7GpppAm (N)_{25'}. Due to the absence of the 5'-5' triphosphate motif, the hybridization probe is observed on both the stainless-steel and low-adsorption flow path.

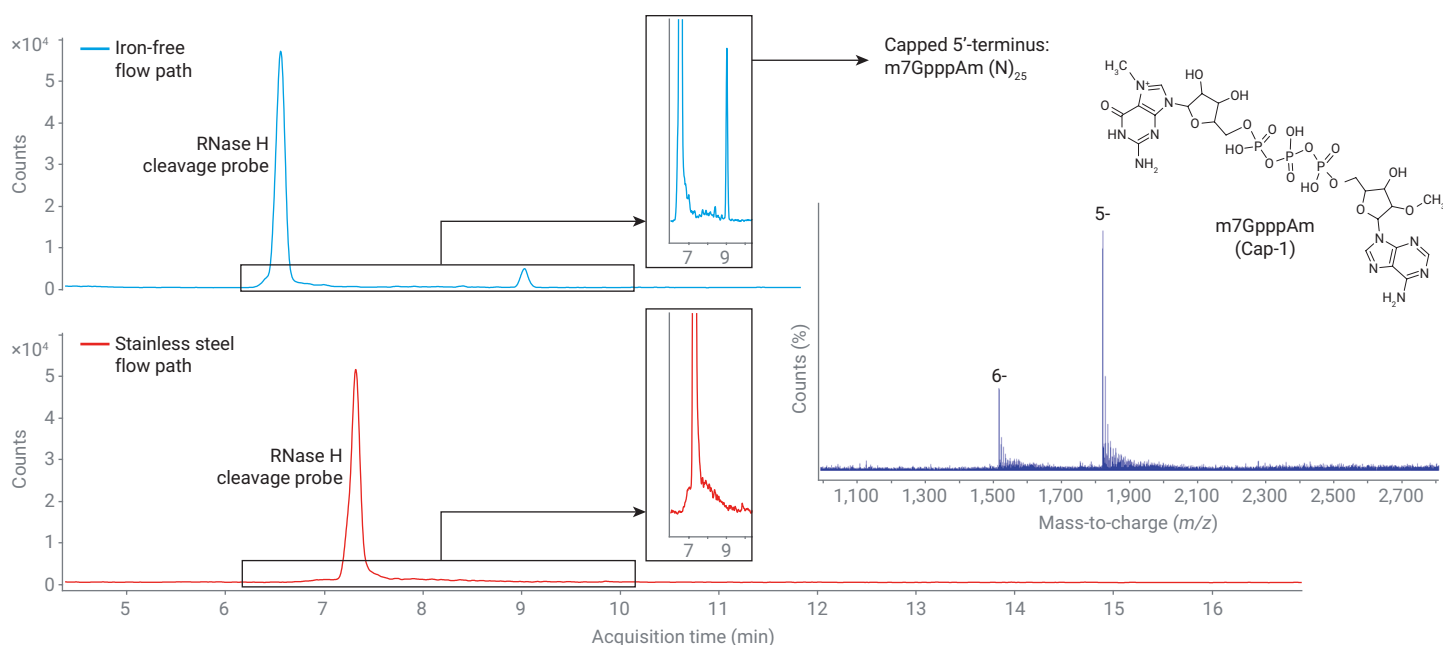


Figure 4. HILIC-MS base peak chromatograms of 5'-terminal Fluc mRNA fragments generated by the RNase H-based method obtained on a iron-free (blue) and stainless-steel configuration (red). The MS spectrum shown in the insert corresponds to the capped 5'-terminus. Gradient 1 (Table 2) was applied.

The RNase A-dependent procedure applied to the 1.2 kb proprietary mRNA, returns both capped (m7GpppAm (N)₆ Cp) and uncapped (A (N)₆ Cp) 5'-terminal fragments as displayed by the HILIC-MS base peak chromatograms (Figure 5). These species, carrying 3' terminal phosphate on top of the internal phosphodiester as a result of RNase A digestion, appear much less intense on the stainless-steel than on the iron-free configuration. Unlike the RNase H procedure, the RNase

A method yields double-stranded molecules in which the hybridization probe remains annealed to the 5'-terminal RNA fragment. HILIC separation at modest temperatures (40 °C here) conserves this RNA/probe double-helical conformation, yet in-source melting might explain their MS spectra, which display m/z peaks for both the single-stranded probe and the 5'-terminal fragment next to those for the RNA/probe double helix (Figure 5).

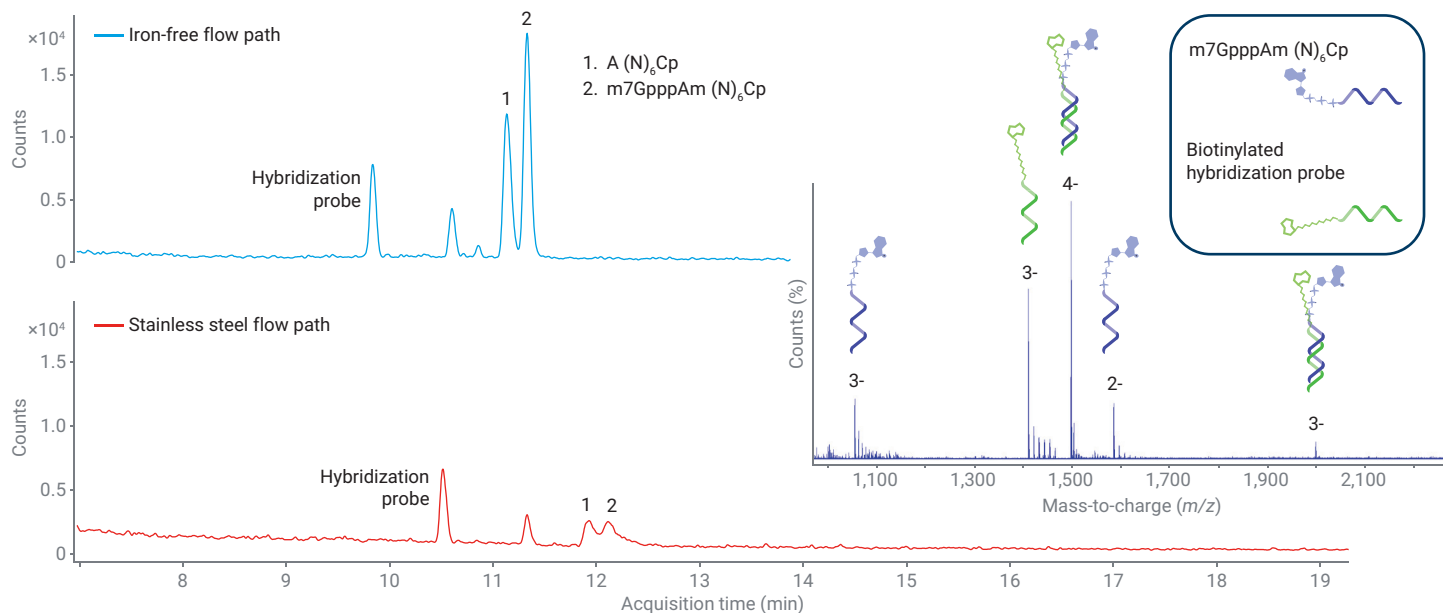


Figure 5. HILIC-MS profiling of 5'-terminal 1.2 kb proprietary mRNA fragments generated by the RNase A-based method. Due to the smaller oligonucleotides encountered, adapted gradient 2 (Table 2) was applied.

Conclusion

The recent tendency to analyze oligonucleotides using LC/MS via HILIC rather than less sustainable IPRP unveils the effect of the iron surfaces in classical stainless-steel columns and systems. Next to a lowered detection sensitivity, peak tailing biases the separation. This peak tailing arises from the internal phosphodiester and, especially, the triphosphates and terminal phosphates of the 5' mRNA fragments. All these phosphate moieties are fully negatively charged above pH 3 and, thus, electrostatically attracted to the iron parts present in both the LC and the column. By employing an Agilent 1290 Infinity II Bio LC and PEEK-lined column, such peak shape distortions and sensitivity losses can be circumvented, paving the way for the unprecedented characterization of IVT mRNA.

References

1. Callaway, E.; Naddaf, M. Pioneers of mRNA COVID Vaccines Win Medicine Nobel. *Nature* **2023**, 622, 228–229.
2. Beverly, M.; Dell, A.; Parmar, P.; Houghton, L. Label-Free Analysis of mRNA Capping Efficiency Using RNase H Probes and LC-MS. *Anal. Bioanal. Chem.* **2016**, 408, 5021–5030.
3. Liao, B. Rapid Analysis of mRNA 5' Capping with High Resolution LC/MS. *Agilent Technologies application note*, publication number 5994-3984EN, **2021**.
4. Morreel, K.; t'Kindt, R.; Debyser, G.; Jonckheere, S.; Sandra, P.; Sandra, K. Diving into the Structural Details of In Vitro Transcribed mRNA Using Liquid Chromatography-Mass Spectrometry-Based Oligonucleotide Profiling. *LCGC Europe* **2022**, 35, 220–236.
5. Nwokeoji, A. O.; Chou, T.; Nwokeoji, E. A. Low Resource Integrated Platform for Production and Analysis of Capped mRNA. *ACS Synth. Biol.* **2023**, 12, 329–339.
6. Wolf, E. J.; Dai, N.; Chan, S. H.; Corrêa, I. R. Selective Characterization of mRNA 5' End-Capping by DNA-Probe Directed Enrichment with Site-Specific Endoribonucleases. *ACS Pharmacol. Transl. Sci.* **2023**, 6, 1692–1702.
7. Guimaraes, G. J.; Kim, J.; Bartlett, M. G. Characterization of mRNA Therapeutics. *Mass Spectrom. Rev.* **2023**, doi: 10.1002/mas.21856.
8. Ramanathan, A.; Robb, G. B.; Chan, S. H. mRNA Capping: Biological Functions and Applications. *Nucleic Acids Res.* **2016**, 44, 7511–7526.
9. Daniel, S.; Kis, Z.; Kontoravdi, C.; Shah, N. Quality by Design for Enabling RNA Platform Production Processes. *Trends Biotechnol.* **2022**, 40, 1213–1228.
10. USP. Analytical Procedures for mRNA Vaccine Quality. USP guideline EA966W_ 2023-04, draft guidelines, second edition. [vaccine-mrna-guidelines-2.pdf \(usp.org\)](#).
11. Huang, M.; Xu, X.; Qiu, H.; Li, N. Analytical Characterization of DNA and RNA Oligonucleotides by Hydrophilic Interaction Liquid Chromatography-Tandem Mass Spectrometry. *J. Chromatogr. A.* **2021**, 1648, 462184.
12. Goyon, A.; Nguyen, D.; Boulanouar, S.; Yehl, P.; Zhang, K. Characterization of Impurities in Therapeutic RNAs at the Single Nucleotide Level. *Anal. Chem.* **2022**, 94, 16960–16966.
13. Li, G.; Rye, P. MS/MS Oligonucleotide Sequencing Using LC/Q-TOF with HILIC Chromatography. *Agilent Technologies application note*, publication number 5994-5632EN, **2023**.
14. Lardeux, H.; Goyon, A.; Zhang, K.; Nguyen, J. M.; Lauber, M. A.; Guilleme, G.; D'Atri, V. The Impact of Low Adsorption Surfaces for the Analysis of DNA and RNA Oligonucleotides. *J. Chromatogr. A.* **2022**, 1677, 463324.
15. Schneider, S. Analysis of Phosphate Compounds with the Agilent 1260 Infinity Bio-Inert Quaternary LC System. *Agilent Technologies application note*, publication number 5991-0025EN, 2012.
16. Sandra K.; Vandenbussche, J.; Vanhoenacker, G.; t'Kindt, R.; Sandra, P.; Krieger, S.; Schneider, S.; Huber, U. Analysis of Nucleotides Using a Fully Inert Flowpath. *Agilent Technologies application note*, publication number 5994-0680EN, **2019**.
17. Schneider, S. Comparability Studies for the Analysis of Nucleotides on Four Different LC Systems. *Agilent Technologies application note*, publication number 5994-4392EN, **2021**.
18. Vanhoenacker, G.; Sandra, P.; Sandra, K.; Schneider, S.; Huber, U. Improving Peak Shape and Recovery in LC Studies of Phosphated Vitamin B2. *Agilent Technologies application note*, publication number 5994-5830EN, **2023**.

www.agilent.com

DE95186582

This information is subject to change without notice.

© Agilent Technologies, Inc. 2024
Printed in the USA, October 15, 2024
5994-7118EN